Experimental studies and mathematical modeling of the curing reaction of bioinspired copolymers

N. Chen, N. Lee, S. A. Bortolato & D. M. Martino

Taylor & Francis
Taylor & Francis Group

Experimental studies and mathematical modeling of the curing reaction of bioinspired copolymers

N. Chen[a], N. Lee[a], S. A. Bortolato[b] and D. M. Martino[c]

[a]Department of Chemistry and Physics, Simmons College, Boston, MA, USA ; [b]Instituto de Química Rosario (IQUIR-CONICET), Rosario, Argentina ; [c]Instituto de Física del Litoral (IFIS-CONICET-UNL), Santa Fe, Argentina

ABSTRACT
Polymer curing is a complex process that significantly delineate the final properties of the synthetized material. In this work, the photo-induced crosslinking reaction of synthetic "bio-inspired" copolymers based on thymine and ionic groups was studied by gel permeation chromatography and UV absorption spectroscopy. A mathematical model for the curing process based on statistical techniques and coupled to the kinetics of crosslinking was developed. The model allows to predict both, the evolution of the crosslinking degree as a function of curing time and the gel times as a function of the molecular structure of the copolymer and the curing conditions. The theoretical values showed a very good agreement with the UV–Vis and GPC spectroscopy experimental results for all the copolymers studied. A better knowledge of the curing kinetics of thymine-based biopolymers will enable to develop materials with pre-specified properties and to improve their applications.
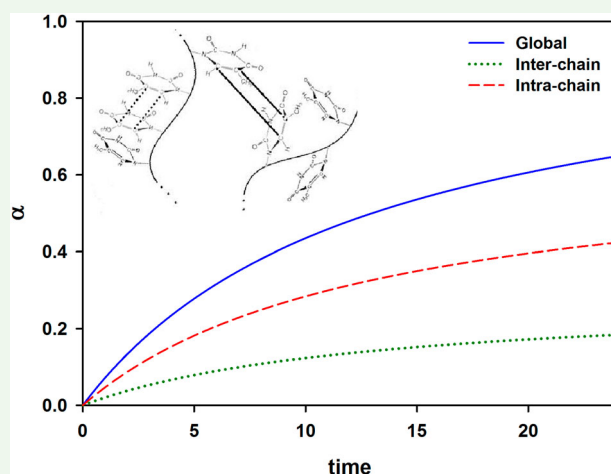
1. Introduction

It is well-known that among the chemical processes in the deoxyribonucleic acid (DNA) chains, the heterocyclic bases of thymine in the sequence may undergo a dimerization reaction with a neighboring thymine in the DNA chain in the presence of ultraviolet (UV) light of short wavelength, $\lambda \sim 280$ nm (1). This reaction produces a crosslinking in the helical structure of DNA leading to cell mutations, a major cause of skin cancer due to excessive exposure to sunlight (2). Inspired by this process, an intense research has been focused to design synthetic polymers containing nucleic acid bases for several years (3). Thymine-containing polymers and supramolecular structures are bio-inspired systems which recently gained much attention due to their photo-sensitivity and molecular recognition patterns (4–7). The 4-vinylbenzyl thymine monomer (VBT), derived from styrene, has the ability to photo-crosslink under UV radiation (8). The homopolymer of VBT is insoluble in water due to the strong intermolecular hydrogen bond interactions between adjacent thymines. However, copolymerizing VBT with ionic monomers, such as vinylbenzyl triethyl ammonium chloride (VBA) or vinylphenyl sulfonate

(VPS), results in water-soluble copolymers, eliminating the use of volatile organic solvents required to treat polymers such as polystyrene.

The adaptability of the VBT monomer that allows for a balance between thymine photo-reactivity, solubility and non-covalent intermolecular interactions has generated a diapason of potential practical applications (9–12) ranging from photo-resists (13,14) and organic-inorganic hybrid devices (5) to antibacterial coatings (15), drug delivery systems (6,16–18), recyclable plastics (19) and biosensors (20,21).

In light of all these possible applications of the copolymer, the rational design of polymeric materials can be enriched by the development of recursive mathematical models that simulate the photo-induced crosslinking (curing reaction) allowing the prediction of the molecular properties of the polymer as a function of the synthetic conditions. The curing reaction is crucial for the application of virtually any polymeric material, hence it is important to absolutely identify the nature of the reaction (22). Polymer curing is a complex process that includes several steps but generally is evidenced by a rapid increase in molecular weight as the reaction progresses since chains are fused in an infinite molecular weight reticulum. The rapid and irreversible transformation in which the polymeric material passes from a viscous liquid to an elastic gel state, indicating the commencement of the reticulum appearance, is often called a ***gel point*** (23).

The gel point is critical in the manipulation of polymeric materials since after this threshold the material stops flowing and cannot be easily controlled. The gelation phenomenon occurs at a specific stage of the reactive process and depends on the functionality, reactivity and stoichiometry of the reactive species. Gelling does not inhibit the curing process (e.g. the reaction rate may not vary), therefore it cannot be detected by techniques sensitive only to chemical reactions, such as differential scanning calorimetry or thermogravimetry (24,25). After gelation, the curing reaction continues until the glass transition temperature and the ultimate physical properties are achieved, forming an infinite lattice with a substantial increase in the crosslink density.

Although the time required for gelation to appear (gel time) should be perfectly defined and easily calculated, its value may vary depending on the interpretation given to the gelation phenomenon. There have been several theories on this matter, although the most successful has been the theory developed by Flory–Stochmayer (26). The current work, started with from Flory–Stochmayer assumptions and inspired by Miller and Macosko recursive models (27,28), proposes an explanation for the curing of bio-inspired thymine-based polymers. Despite the relevant impact of the curing process

on the polymer's final properties, the complexity of having reliable estimates on the reaction evolution precludes the development of efficient mathematical models and is a challenge in the polymer science.

In this study, the curing of two VBT-VBA copolymer coated on a polyethylene terephthalate (PET) film substrate was carried out by irradiation at 254 nm, which causes a photo-cyclodimerization reaction within the copolymer and lead to an immobilization on the substrate (29). As the exposure time increases the number of crosslinks connecting the polymer chains increases, and eventually, the density of crosslinks reaches the critical point when insoluble "infinite" molecular weight networks are formed, leading to a decrease of VBT-VBA copolymer absorbance at 270 nm in the washed solution. This process will result in the determination of the gel point using Gel Permeation Chromatography (GPC) with a UV detector.

Furthermore, an indirect measurement of the crosslinked copolymer on the film can be measured by toning the substrate after irradiation with an anionic dye (30). The anionic dye has low affinity toward PET film, however, it is readily attracted to the opposite charged VBT-VBA copolymer coated on the film, through electrostatic interactions. The absorbance of the anionic dye attached to the film containing crosslinked copolymer should increase as the irradiation time grows due to an increase in the photo-crosslinking degree, and this process was studied using UV–vis spectrophotometry.

Finally, a mathematical model for the curing process of photo-induced crosslinking reactions was developed in order to predict the evolution of the crosslinking degree as a function of irradiation time, and the gel time as a function of the polymer molecular structure and the curing conditions. The crosslinking process was monitored as a function of irradiation time via gel permeation chromatography and UV absorption spectroscopy, and experimental results were compared to theoretical data obtained with the developed mathematical model. The central goal is to optimize the synthesis and curing kinetics of thymine-based copolymers to get materials with pre-specified properties and quality, and correspondingly improve their applications.

2. Theory: mathematical model

Under well-known experimental conditions (polymerization procedures, initiator concentration, coating conditions, irradiation dose, developing/washing method, etc.), the photo-induced crosslinking process within the copolymer can be monitored as a function of irradiation time and simulated mathematically. UV irradiation does

not modify the VBA monomer, while it induces the thymine moiety to react with other neighbor thymine, leading to crosslinking of the chains (31). Consequently, the crosslinking degree "**α**" can be defined as follows:

$$\alpha = \frac{[Ty]_0 - [Ty]}{[Ty]_0} = 1 - \frac{[Ty]}{[Ty]_0}, \qquad (1)$$

where $[Ty]_0$ is the initial concentration of thymine, and $[Ty]$ is the thymine concentration at each time, both obtained from the UV absorption and GPC spectra of the washed solution.

The mathematical model for the curing process consists of two modules, a **Kinetic module (KM)** and a **Statistical module (SM)**. The **KM** relates the degree of crosslinking **α** with the irradiation time and the curing conditions. The **SM** is based on the crosslinking model of chains with molecular weight distribution and functionality known from Miller and Macosko (27,28) that allows calculating the molecular weights as a function of **α**.

The **KM** considers that the crosslinking process is a second order reaction with respect to the molar concentration of thymine ([Ty]) (31). Thus, the evolution of thymine concentration can be found from the following balance:

$$\frac{d[Ty]}{dt} = -k[Ty]^2. \qquad (2)$$

In Equation (2), **k** is the kinetic constant of the curing reaction at 254 nm and its value is 1030 L mol^{-1} s^{-1} (31). Integrating Equation (2) from 0 to t, and considering Equation (1), the degree of crosslinking is defined as follows:

$$\alpha(t) = 1 - \frac{1}{[Ty]_0\ kt + 1}. \qquad (3)$$

Finally, coupling Equation (3) with the results of the statistical module, it is possible to estimate the evolution of the molecular weights versus irradiation time. It is worth noticing that the balance presented in Equation (3) is valid only for reactions without diffusional effects. In our systems, the crosslinking reaction is accomplished when copolymers are coated on thin films, therefore diffusional effects can be negligible.

For the **SM**, in the beginning, it was considered that the Flory–Stockmayer assumptions for the formation of crosslinked networks were met (26), namely: (1) all functional groups are equally reactive, (2) all functional groups react independently and (3) intra-chain or intra-molecular reactions do not exist. Additionally, from the measurements of the composition during the synthesis reaction it was determined that the monomers were randomized (32). Therefore, a random distribution of reactive sites (i.e. VBT units) was assumed. Under these assumptions, according to Miller and Macosko, the model for homo-polymerization leads to the following fundamental equation to calculate the weight-average molecular weight ($\bar{M}_w$) as a function of **α**:

$$\begin{aligned} \bar{M}_w = {}& \bar{m}\bar{L}_w + \frac{\alpha\, p\, \bar{m}\, \bar{L}_w^2}{1 - \alpha\, p\, (\bar{L}_w - 1)} \\ & + (\Delta m\, (1 - p)\, p)\frac{2\alpha\, \bar{L}_w + (1 + \alpha - \alpha\, p\, \bar{L}_w)\Delta m/\bar{m}}{(1 - \alpha\, p\, (\bar{L}_w - 1))}. \end{aligned}$$

$$(4)$$

In Equation (4), m is the weight of reactive repeat unit chain (VBT), $\bar{L}_w$ is the weight-average number of repeat units in chain, Δm is the weight difference between non-reactive (VBA) and reactive units, and p is the proportion of repeat units with reactive sites which indicates the probability that a randomly chosen repeat unit holds a reactive site. The innovation in this approach is that the degree of crosslinking "α" in Equation (4) is obtained with Equation (3), and consequently, in our model, the kinetics and the statistics of the curing process can be coupled.

When analyzing the outcomes of the simulations based on the coupled model synthesized in Equation (4), severe discrepancies have been detected. The observed discrepancies between the theoretical values of gel point calculated with the **SM** and the experimental data can be attributed to the presence of intra-chain reactions, causing the advancement of the curing reaction without an increase in molecular weight of the copolymer.

Consequently, in order to consider the intra-chain reactions and explain the discrepancies, the **SM** was extended. In the **Extended Statistical Module (ESM)**, a conditional matrix based on a Monte Carlo approach was introduced to simulate the intra-molecular reactions, modifying the prediction of the copolymers weight-average molecular weight ($\bar{M}_w$) evolution (33–35). The key is to generate a special matrix displaying a scenario that considers thousands of unequal polymer chains. A mathematical array matrix called *cell array* and represented by { } have been used, being a collection of independent column-matrices, as shown in Equation (5):

$$A = \left\{ \begin{bmatrix} 0 \\ 1 \\ 0 \\ 1 \\ 1 \end{bmatrix} \begin{bmatrix} 1 \\ 0 \\ 1 \end{bmatrix} \begin{bmatrix} 0 \\ 0 \\ 1 \\ 0 \\ 1 \\ 1 \\ 0 \\ 1 \end{bmatrix} \begin{bmatrix} 0 \\ 1 \\ 1 \\ 0 \\ 0 \end{bmatrix} \right\}. \qquad (5)$$
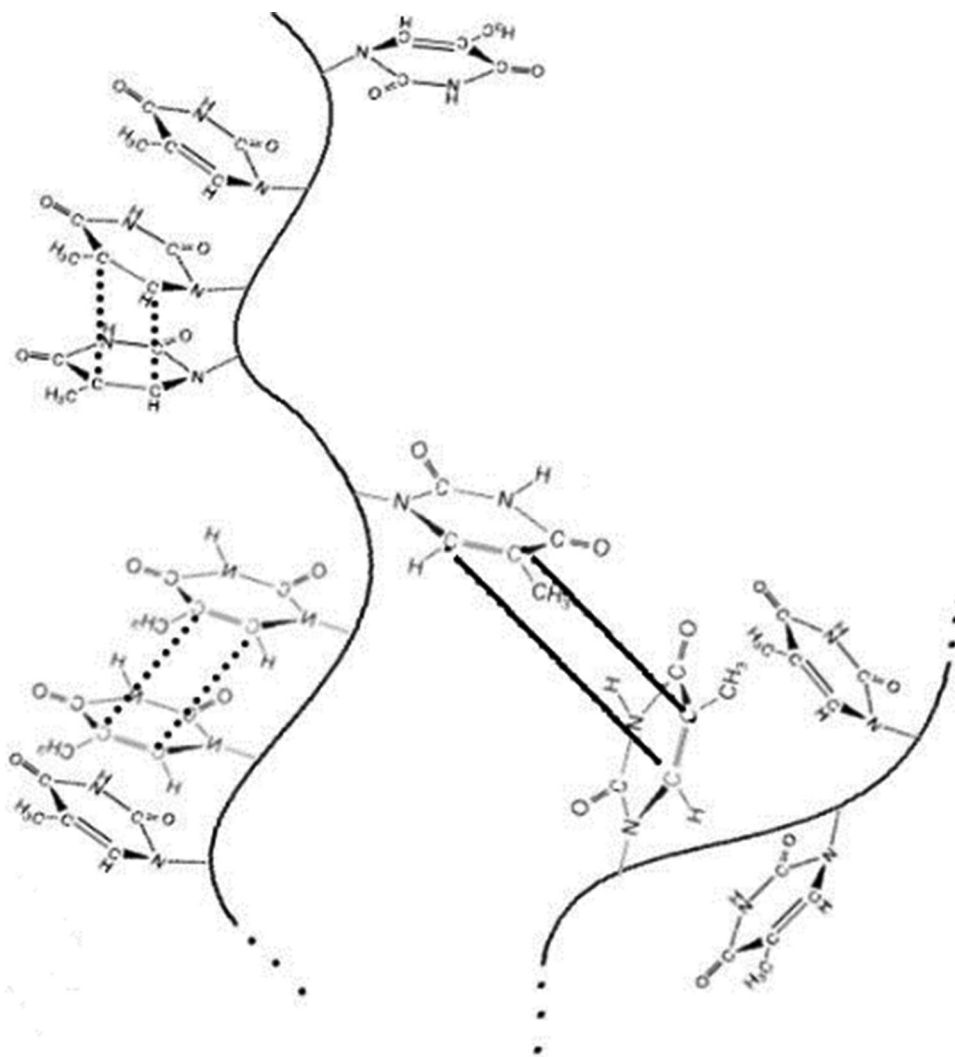
Figure 1. Copolymer chains showing crosslinking inter-chain (solid lines) and intra-chain interactions (dotted lines). The ESM model allows to discriminate them through a special matrix to better predict the curing kinetics.

Such a matrix, labeled "**A**" in the example, provides the following vital information: (a) total number of chains (i.e. 4 in matrix **A**) that can reach thousands in our real case; (b) length of independent chains (i.e. (5,3,8,5) in matrix **A**) and (c) sequence length distribution. Assigning 1 to VBT monomer and 0 to VBA monomer, and in view of chain 3 (longest chain in matrix A), the program scans for the chosen sequence and gives the following dyads: (0–0) = VBA-VBA, (1–0) = VBT-VBA, (1–1) = VBT-VBT, and (0–1) = VBA-VBT. Consequently, the dyads, triads, etc. can be easily identified since the program accesses each element within every chain. In particular, it is important to emphasize that the third dyad (1–1) represents precisely the intra-chain type of interaction that increases the degree of crosslinking and does not lead to an increase in molecular weight. The addition of this cell array allows the algorithm to separate the intra-chain interactions from the evolution of the degree of reaction. The correction of the curing kinetics is completed by neglecting intra-chain interactions, randomly simulated from a Monte Carlo-type strategy, and allowing interactions between 1's aligned in neighboring dyads to essentially occur. Figure 1 shows schematically the situation previously described.

The *cell array* is used at the beginning of the algorithm and then updated as the simulated curing reaction progresses according to the model summarized in Equation (4). In consequence, the growth of the chains does not artificially modify the possibilities of non-contributory interactions.

The mathematical models were implemented in MATLAB (36). A typical simulation lasted less than 3 minutes on a PC microprocessor Athlon X2 Dual-Core QL-60 (1.90 GHz).

3. Experimental details

3.1. Materials

Thymine, 4-vinylbenzyl chloride (VBC), 2,2′-azobisisobu-tyronitrile (AIBN), Inhibitor 3,5-di-tert-butyl-4-hydroxyto-luene (BHT), Triethylamine (TEA), Toluene, Methanol (HPLC grade), Acetic acid, FD&C and Erythrosine B were purchased from Sigma-Aldrich. Ethanol (95%), Isopropa-nol (99%, ACS) and Acetone (99.9%) were purchased from Pharmco-Aaper. Sodium hydroxide (99%) was pur-chased from Fisher Scientific and Dimethyl formamide (DMF, 99.8%) from VWR. Ethyl acetate (ACS grade) and Hexanes (ACS grade) were purchased from Macron. Water (HPLC grade) was purchased from Spectrum. Deuterated DMSO (99.9%) and Deuterium oxide (D_2O, 99.96%) were purchased from Cambridge Isotope Lab-oratories. Poly 2-Vinylpyridine (PVP) polymer standards were purchased from Jordi Labs. All reagents were used as received unless mentioned otherwise.

Monomers and copolymers were dried using a VWR® 1410 Vacuum Oven (T: 80°C, pressure: 28 inHg). Degasification of isopropanol was performed using Branson®1510 Tabletop Ultrasonic Cleaner Sonicator.

^{1}H NMR analysis of monomers and copolymers were performed using Anasazi EFT 90 MHz NMR spectrometer and IR studies were performed using Varian Scimitar FTS-800 FT-IR Spectrophotometer.

GPC experiments were performed using Beckman System Gold Programmable Solvent Module (126) HPLC system with an UV/Vis Programmable Detector Module (166). A guard column (Jordi DVB Polar Pack Wax mixed bed, 50 mm × 10 mm, 5 micron particles) and two analytical columns (Jordi DVB Polar Pack Wax mixed bed, 250 × 10 mm, 5 micron particles) were pur-chased from Jordi Labs. Copolymer solutions were filtered through a WHATMAN 0.45 μm filter attached to a BD 1mL Luer-Lok tip syringe before sample injection. GPC mobile phase filtration apparatus was purchased from Quark Glass. Average molecular weight determi-nation and peak integrations were performed using Scientific Information Service Cooperation (SISC-32) Chromatography Data Station.

3.2. Synthesis of sodium thyminate

Sodium hydroxide (2.04 g, 0.051 mol) was added to a round bottom flask containing 30 mL of DI water. The solution was heated to 50°C and stirred at 300 RPM until dissolved. Thymine (6.50 g, 0.044 mol) was added and stirred for additional 20 min. After the solution has completely turned clear, the flask was removed from heat and cooled to room temperature for 10 min. Ethanol (50mL) was added slowly to the stirring solution

and a white precipitate was observed. The white solid was filtered and dried overnight in a vacuum oven at 80°C under 25 inHg vacuum. Sodium thyminate col-lected (3.80 g, 49.85% yield) was characterized to confirm its identity and purity using both FT-IR and ^{1}H NMR spectroscopy.

3.3. Synthesis of 4-vinyl benzyl thymine (VBT)

Sodium thyminate (15.75 g, 0.106 mol) was added to 80 mL DMF in a round bottom flask and stirred. Once the solution turned clear, a mixture solution of VBC (9.57 g, 0.063 mol) and inhibitor BHT (0.026 g, 1.18 × 10^{-4} mol) was added. The flask was placed in a 70°C hot oil bath with a reflux condenser attached and stirred for three hours, forming a light yellow opaque mixture. The DMF solvent was removed via rotary evap-oration under vacuum. The solvent free flask containing the reaction mixture was then placed into an oil bath pre-heated to 110°C. About 120 mL of boiling toluene was added gradually to the flask until no more solid was dissolved. A hot vacuum filtration was performed using pre-heated ceramic funnel. After filtration, the clear, yellow liquid filtrate was allowed to cool to room temperature and a white precipitate was observed. The flask was then placed in an ice bath and allowed to cool for 30 min, where more white precipitates were formed. The mixture was then vacuum filtered and rinsed with ice-cold toluene. The final product (5.73 g, 36.30% yield) was purified using a Teledyne Isco Combi-Flash Rf 200 and characterized by ^{1}H NMR.

3.4. Synthesis of 4-vinyl(benzyl) triethyl ammonium chloride (VBA)

In a single neck round bottom flask, acetone (75 mL) was added and heated to 60°C with stirring at 450 RPM. TEA (6.65 g, 0.066 mol) was added to the stirring acetone, fol-lowed by adding VBC (9.97 g, 0.066 mol) drop wise. A yellow clear solution was observed. With a condenser attached to the flask, the reaction mixture was refluxed at 60°C for one hour, and then allowed to cool at room temp-erature overnight with no stirring for crystal growth. The crystalline product was filtered using vacuum filtration and rinsed with cold acetone. The final crystals were dried in the vacuum oven at 80°C under 25 inHg vacuum overnight (4.82 g, 28.92% yield), and characterized to confirm purity using 1H NMR spectroscopy.

3.5. Synthesis of VBT:VBA$_4$ copolymer

Synthesis of the copolymer (0.4% AIBN). In a three neck round bottom flask equipped with a stirring bar and

nitrogen inlet, finely ground VBT (1.023 g, 4.22×10^{-3} mol) was dissolved in 40 mL degassed isopropanol in 85°C oil bath. Once a white, opaque liquid was observed, finely ground VBA (4.34 g, 1.71×10^{-2} mol) was dissolved in 30 mL degassed isopropanol and added into VBT solution with stirring at 950 RPM. Once the reaction mixture has turned translucent and colorless, the temperature of the reaction was lowered to 65°C and AIBN (0.022 g, 1.32×10^{-4} mol, 0.40% w/w) dissolved in 2 mL of degassed isopropanol was added. The reaction was run for 18 h under nitrogen. After 18 h, a clear solution was observed, the temperature was turned off and the reaction was allowed to cool down to room temperature with stirring for an additional 2 h. The copolymer was isolated from the reaction mixture via precipitation in 500 mL acetone. The final product was vacuum filtered and dried in a vacuum oven overnight at 80°C under 25 inHg vacuum (4.95 g, 98.98% yield) and its purity was confirmed by ^{1}H NMR.

Synthesis of VBT:VBA$_4$ copolymer (1.0% AIBN). The same procedure was followed, only changing the amount of AIBN added (0.054 g, 3.26×10^{-4} mol, 1.00% w/w). The final product (4.54 g, 90.91% yield) was characterized by ^{1}H NMR.

3.6. Gel permeation chromatography (GPC)

Molecular weights of the synthesized VBT:VBA$_4$ copolymers as well as their gel point were determined by GPC experiments. A guard column and two analytical columns in series were used. A 70/30 water/methanol with 1M acetic acid solution was used as the mobile phase and sample diluent. The mobile phase was vacuum filtered with Nylon 66 membrane (0.45 μm × 47 mm, Supelco). Four poly(2-vinyl pyridine) polymers (PVP) with molecular weights 1910, 20,500, 41,700, 245,000 were used as references. A 0.10% w/w solution of each standard was prepared using the mobile phase as solvent. A mixture of the four different molecular weights was filtered and used to generate the M_w calibration curve of the PVP standard polymer.

A 0.25% w/w of VBT:VBA$_4$ copolymer solution was prepared using the eluting solvent. The copolymer solutions were wrapped with aluminum foil to avoid light contact and placed on an Orbital Shaker (Orbit300, Labnet International Inc.) overnight resulting in a clear, colorless, viscous polymer solution. Each solution was filtered before injection.

GPC experiments were run at a sampling rate of 10 pts/sec, for a total run time of 60 min. A flow rate of 1 mL/min was used for all runs monitoring changes at 270 nm wavelength. During sample injection, 15 μL of standard mixture solution was injected into the

column, followed by individual VBT-VBA copolymer samples.

3.7. Copolymer coating

A 10% (w/w) solution of VBT:VBA$_4$ ratio was prepared by dissolving 0.308 g of VBT-VBA copolymer in 2.78 g of 50/50 w/w ethanol/DI water solution. The solution was agitated on an orbital shaker at 300 RPM for 24 h to ensure all the copolymer dissolved. The final copolymer solution was colorless, clear liquid and slightly viscous.

400 μL of the 10%w/w VBT:VBA$_4$ copolymer solution in 50/50w/w water/ethanol were coated onto a pre-treated PET film (10.5 cm × 28.0 cm Melinex 454/500, DuPont Teijin Films) using a wire-rounded #3 Mayer rod (R. D. Specialties, Webster, NY) leaving a thin, uniform film. The coated film was dried for 3 h at room temperature followed by drying in the oven at 80°C and cut into equal size rectangles of 1.6 × 3 cm^2. The films were irradiated at 254 nm using the Spectroline® E-series Ultraviolet Hand Lamp (Spectronics Corporation, Westbury, NY) from a distance of 1.2 cm, for irradiation times of 0, 5, 10, 15, 20, 25, 30, 35,40, 60, 80, 100 and 120 s. After irradiation, each rectangle piece was washed for 1 min in 1 mL of GPC mobile phase. The process was repeated for five PET films for each irradiation time to ensure a concentrated sample for GPC experiment. For each irradiation time, 0.5 mL of copolymer washed solution was placed into 0.7 mL quartz micro cuvette (Precision Cells) to follow the absorbance at 268 nm (Agilent 8453 Diode Array UV–Vis Spectrophotometer) and the remaining solution was used for GPC measurements. GPC mobile phase was used as blank.

For the indirect measurement of the copolymer cross-linking, the irradiated films were toned in 1 mL of 5% FD&C dye (VBT:VBA$_4$ 0.4% AIBN) or 1 mL of 1 mM Erythrosine B (VBT:VBA$_4$ 1.0% AIBN) with gentle shaking after being washed with GPC mobile phase. For each irradiation time, the UV–Vis absorbance at 501 nm for FD&C or 545 nm for Erythrosine B was collected.

4. Results and discussion

VBT was copolymerized with VBA via free-radical polymerization with AIBN as an initiator. From the ^{1}H NMR spectra, the disappearance of vinyl groups (doublet of doublet peaks) between 5 and 6 ppm for both 0.4% AIBN and 1.0% AIBN VBT:VBA$_4$ copolymers indicates the absence of the monomers in the copolymer samples.

The resulting VBT:VBA$_4$ copolymers not only retained the ability to photo-crosslink upon irradiation with short-
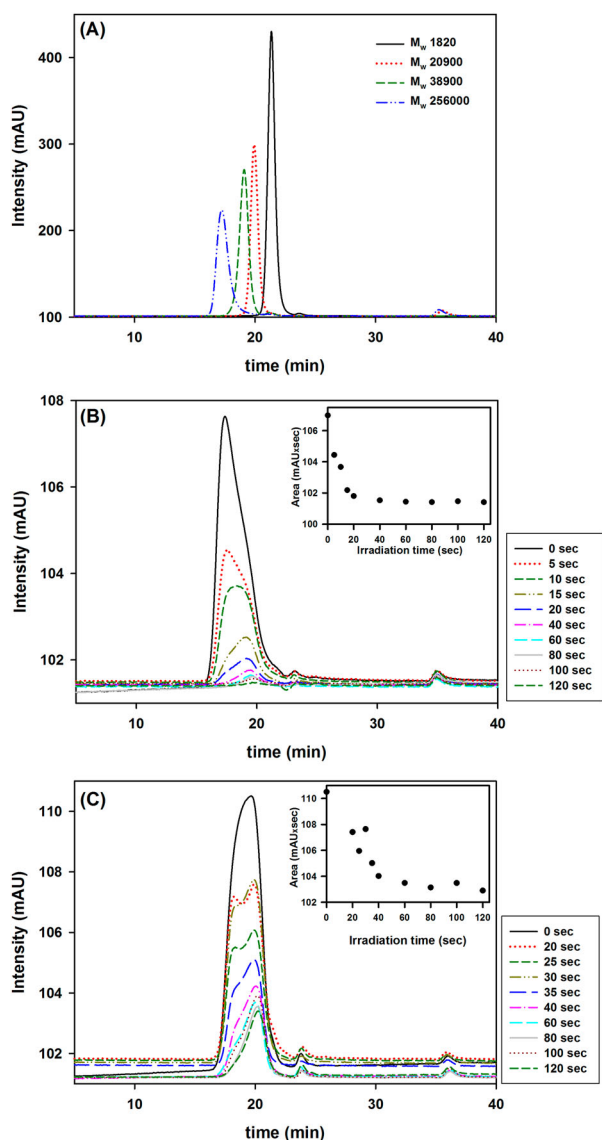
Figure 2. GPC chromatograms. (A) Mixture of GPC standards (retention times: 21.36, 19.92 , 19.10, 17.42 min), (B) Washed solutions of VBT:VBA4 copolymer 0.4% AIBN (retention time 17.83 min) and (C) VBT:VBA4 copolymer 1.0% AIBN (retention time 19.36 min) at various irradiation times. Inset: Area under the GPC peak as function of irradiation time.

wavelength UV light, but also gained the property of being water-soluble from the cationic VBA. When VBT: VBA$_4$ copolymers are irradiated at 254 nm, the thymine groups of adjacent VBT molecules dimerize through the photo-dimerization site, resulting in covalent cyclobutane rings.

4.1. Molecular weight measurement

Figure 2 shows the GPC chromatograms of the four PVP standards of molecular weights 1820, 20,900, 38,900 and 256,000 used to create the calibration curve (Figure 2(A)), and the washed solutions of synthetized VBT:VBA$_4$

Table 1. Weight-average molecular weight and molecular weight distribution for two different VBT:VBA$_4$ copolymers.

VBT:VBA$_4$ copolymer	RT (min)	M_p	M_n	M_w	PDI
0.4% AIBN	17.83	152,000	19,900	135,000	6.78
1.0% AIBN	19.36	32,500	20,000	68,000	3.40

copolymers with 0.4% AIBN (Figure 2(B)) and 1.0% AIBN (Figure 2(C)) at various irradiation times (representing non crosslinked copolymers). The peaks of the standards appeared at expected retention times and therefore are suitable to predict the copolymers molecular weights. The retention times of the VBT:VBA$_4$ copolymers were determined to be 17.83 min for 0.4% AIBN and 19.36 min for 1.0% AIBN.

Table 1 shows the calculated weight-average molecular weights (M_w) for both VBT:VBA$_4$ copolymers. The 0.4% AIBN VBT:VBA$_4$ copolymer was determined to have higher molecular weight compared to the 1.0% AIBN copolymer, in agreement with a lower concentration of AIBN initiator used during the polymerization process, which lead to less initiation points and therefore higher molecular weight chains. However, the polydispersity index (PDI) value of the 0.4% AIBN copolymer was larger than the 1.0% AIBN copolymer, indicating a wider molecular weight distribution compared to the 1.0% AIBN copolymer.

4.2. Gel point determination

4.2.1. VBT:VBA$_4$ copolymer (0.4% AIBN)
Figure 3 shows the UV–Vis spectra of the VBT:VBA$_4$ copolymer (0.4% AIBN) washed solution at various irradiation times using the procedures described in the experimental section (3.6). It can be observed that the absorbance of the peak at 270 nm decreases as the irradiation time increases, indicating that the amount of copolymer in the washed solution decreased with increasing
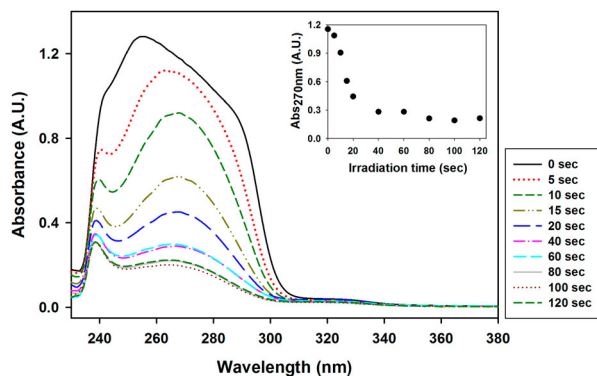

Figure 3. UV–Vis spectra of the VBT:VBA$_4$ copolymer (0.4% AIBN) washed solution at various irradiation times. Inset: Evolution of the absorbance at 270 nm as function of irradiation time.
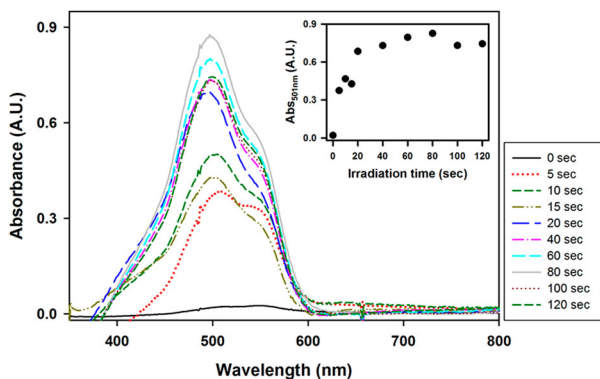
Figure 4. UV–Vis spectra of VBT:VBA$_4$ copolymer (0.4% AIBN) irradiated films toned with FD&C after the washing process at various irradiation times. Inset: Evolution of the absorbance at 501 nm as function of irradiation time.

Figure 6. UV–Vis spectra of VBT:VBA$_4$ copolymer (1.0% AIBN) irradiated films toned with Erythrosine B after the washing process at various irradiation times. Inset: Evolution of the absorbance at 545 nm as function of irradiation time.

irradiation times. This observation was expected since as irradiation time increases, the amount of crosslinked copolymer increases as well, becoming water insoluble and remaining on the substrate. From the graph of the absorbance value at 270 nm versus irradiation times (inset Figure 3), it can be estimated that the gel point of the VBT:VBA$_4$ copolymer (0.4% AIBN) occurs between 20 and 40 s of irradiation.

Figure 4 shows the UV–Vis spectra of VBT:VBA$_4$ copolymer (0.4% AIBN) irradiated films toned with the anionic dye FD&C Red No 3 after the washing process. The inset of Figure 4 shows the evolution absorbance at 501 nm as function of the irradiation time. An increase in the absorbance of the FD&C dye intensity was observed between 0 and 20 s, as expected due to the intensification of crosslinked copolymer remaining on the film with increasing irradiation time. After 20 s, the absorbance values remained constant, suggesting that the copolymer reaches saturation at 20 s.

Figure 2(B) shows the GPC chromatogram of the washed solution of VBT:VBA$_4$ copolymer (0.4% AIBN) at
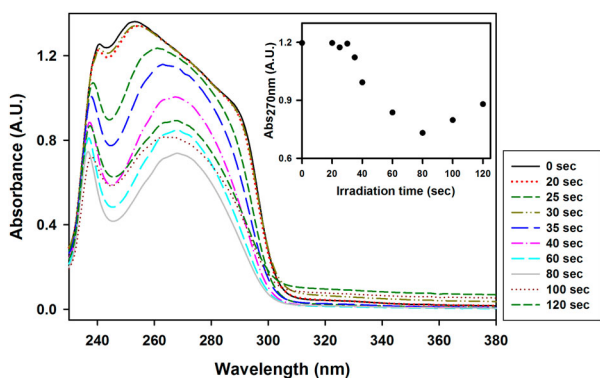
various irradiation times where the intensity of the peak decreases as irradiation time increases, having the same trend as the UV–Vis result of the washed solution (Figure 3). From the chromatogram, no extra peaks were observed at any irradiation time, however, a peak broadening was observed after 10 s of irradiation simultaneously with a shift of the peak to a longer retention time. The broadening and shifting of the peak might be an indication of different copolymer chains with different molecular weight forming in the solution after 10 s of irradiation, and the molecular weight difference might not be large enough for these copolymers to be resolved into two separate peaks. Since the GPC measurements were done using a UV–Vis detector, the area under the peak can be used as a concentration indicator. The graph of area versus irradiation time (inset Figure 2(B)) shows a decrease with increasing irradiation time, indicating that the concentration of the VBT:VBA$_4$ copolymer (0.4% AIBN) in the washed solution drops as irradiation time increases, similar to UV–Vis results.

4.2.2. VBT:VBA$_4$ copolymer (1.0% AIBN)

Figure 5 shows the UV–Vis spectra of the VBT:VBA$_4$ copolymer (1.0% AIBN) washed solutions at various irradiation times. The absorbance at 270 nm versus irradiation time, inset Figure 5, showed a minimal decrease between 0 and 35 s of irradiation and started to change afterwards, suggesting that the gel point of the VBT:VBA$_4$ copolymer (1% AIBN) occurs after 35 s of irradiation.

Figure 6 shows the UV–Vis spectra of VBT:VBA$_4$ copolymer (1.0% AIBN) irradiated films toned with Erythrosine B after the washing process. The inset of Figure 6 shows the evolution absorbance at 545 nm as function of the irradiation time. An increase in the absorbance of the Erythrosine B dye intensity was observed between 0 and 40 s, as expected due to

Figure 5. UV–Vis spectra of the VBT:VBA$_4$ copolymer (1.0% AIBN) washed solution at various irradiation times. Inset: Evolution of the absorbance at 270 nm as function of irradiation time.
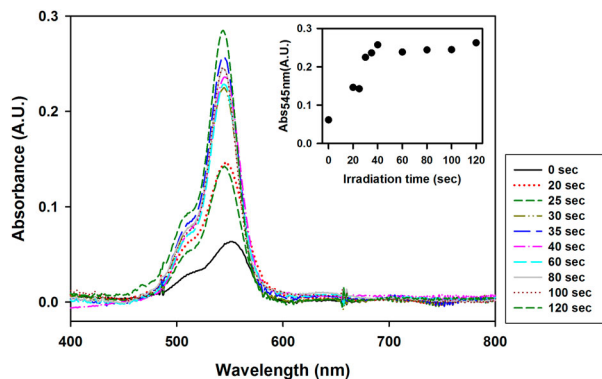
Table 2. Parameters used to evaluate the KM/ESM model.

Parameters	Values
VBT molecular weight	242.28 g mol^{-1}
VBA molecular weight	253.82 g mol^{-1}
$[Ty]_0$	3×10^{-5} L mol^{-1}
Functionality	4
Number average molar weight ($\bar{M}_n$)[a]	
0.4%AIBN	19,900 (Da)
1.0%AIBN	20,000 (Da)
Weight-average molar weight ($\bar{M}_w$)*	
0.4%AIBN	135,000 (Da)
1.0%AIBN	68,000 (Da)
Distribution of reactive sites	Random
Kinetic constant	1030 L mol^{-1} s^{-1}

[a]Initial molecular weights experimentally obtained.

the intensification of crosslinked copolymer remaining on the film with increasing irradiation time. After 40 s, the absorbance values remained constant, suggesting that the copolymer reaches saturation in the region of 40 s.

Figure 2(C) shows the GPC chromatogram of the washed solution of VBT:VBA$_4$ copolymer (1.0% AIBN) at various irradiation times where the intensity of the peak decreases as irradiation time increases, having the same trend as the UV–Vis result of the washed solution (Figure 5). From the chromatogram, no extra peaks were observed for any irradiation time, however, separations of the peak were observed after 40 s of irradiation, followed by a peak shifting. The separation and shifting of the peak might again, be an indication of a different copolymer species with different molecular weight forming in the solution after 35 s of irradiation.

4.2.3. Molecular weight calculations

As the VBT:VBA$_4$ copolymer crosslinks, the length of the copolymer chain extends, causing an increase in the copolymer molecular weight and therefore, changing the characteristics of the VBT:VBA$_4$ copolymer from water-soluble to water insoluble. It was predicted that during the crosslinking process, when the copolymer reaches its gel point, the molecular weight will tend to infinity.

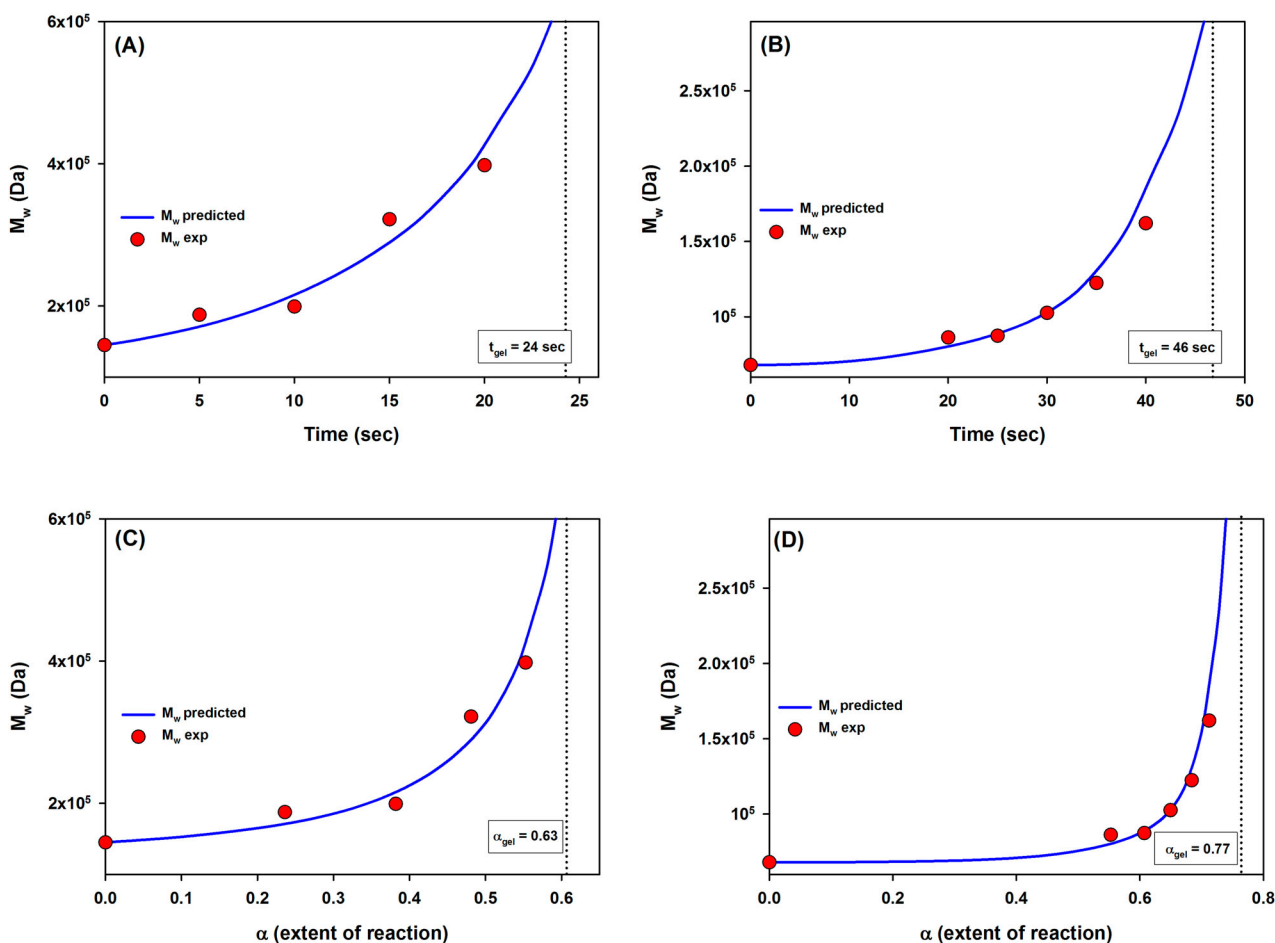The molecular weight of the copolymer as function of time after irradiation was calculated using a

Figure 7. Molecular weight evolution as function of time (A, B) or extent of reaction (C, D) for the VBT:VBA$_4$ copolymer. (A and C) 0.4% AIBN, (B and D) 1.0% AIBN. Red dots indicate the experimental values found, while blue solid lines show the mathematical model predicted molecular weights for both copolymers. Dotted lines indicate the corresponding gel point times (t_{gel}) and gel points (α_{gel}).

mathematical model that takes into account the approximate concentration of the crosslinked copolymer remaining on the film after irradiation, the area under the peak of the chromatogram of the washed solution at different irradiation times, and the initial molecular weight of the copolymer to calculate the molecular weight of the crosslinked copolymer after each irradiation time, as explained in theory section (2.1). This model also takes into account the presence of two types of crosslinking processes taking place within the copolymer: inter-chain and intra-chain crosslinking processes, as explained in the theory section. During the inter-chain crosslinking process, the thymine moieties of one copolymer chain crosslinks with the adjacent thymine corresponding to a different copolymer chain, causing an increase in the molecular weight of the copolymer. However, during an intra-chain crosslinking process, the thymine moieties of one copolymer chain crosslinks with the adjacent thymine in the same chain, which will not result in an increase of the copolymer molecular weight. Table 2 shows the parameters used in the model and the corresponding values in the calculations. Parameters have been previously explained in Section 2.

Figure 7(A) presents the molecular weight evolution as function of time for the VBT:VBA$_4$ copolymer (0.4% AIBN) after each irradiation time from 0 to 25 s. The graph shows the predicted molecular weight from the model (blue solid line), and the molecular weight from experimental data (red dots). The molecular weight of the copolymer from each irradiation time was computed using the molecular weight of the previous irradiation time. The initial thymine concentration at irradiation time 0 is referred as the starting concentration of the thymine on each PET film, and was calculated by taking the amount of copolymer solution coated on the film divided by the total pieces of rectangle obtained from the coated film, and then washed in 1mL of GPC solvent. The concentration of thymine in the solution after irradiation was calculated by taking a proportion of the initial concentration and absorbance.

From the graph shown in Figure 7(A), it was observed that the molecular weight increases exponentially approaching to infinity with increasing irradiation times from 0 to 25 s. It was determined that the gel point of the VBT:VBA$_4$ copolymer (0.4% AIBN) occurred at $t_{gel} = 24$ s of irradiation, as the molecular weight gets positive infinity after this point. Since the mathematical model is not compatible with crosslinked copolymers after the gel point, the rationalization of the copolymer behavior after 35 s of irradiation was not studied in this experiment.

Figure 7(B) shows the molecular weight evolution in function of time for the VBT:VBA$_4$ copolymer (1.0% AIBN) for each irradiation time from 0 to 50 s using the
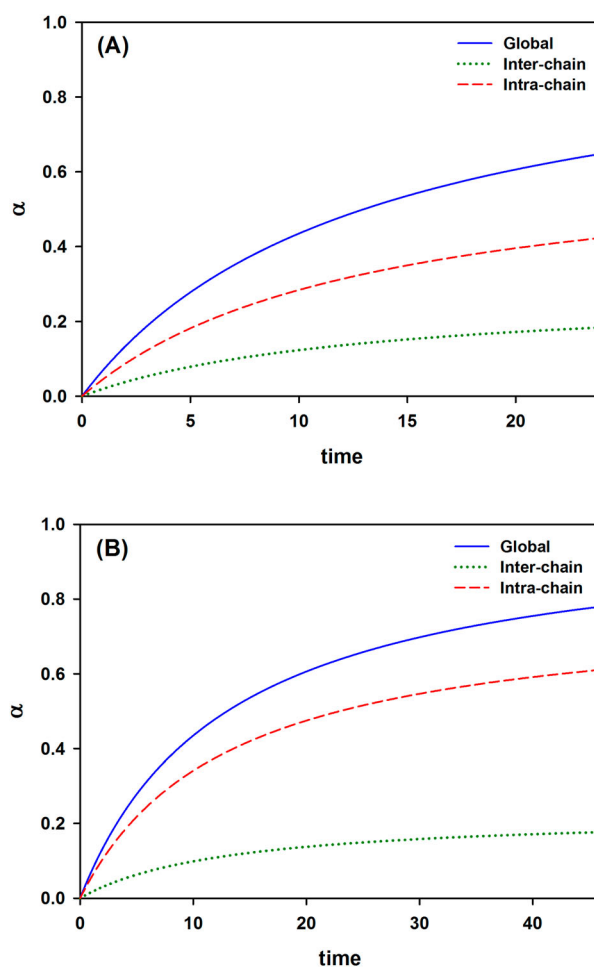

Figure 8. Contribution from inter- and intra-chain crosslinking reactions, according to the mathematical model developed: (A) VBT:VBA$_4$ copolymer (0.4% AIBN) and (B) VBT:VBA$_4$ copolymer (1.0% AIBN).

same method described for VBT:VBA$_4$ copolymer (0.4% AIBN). From the graph, it was observed that the molecular weight increases exponentially approaching to infinity with increasing irradiation times from 0 to 50 s, and it was calculated that the gel point for the VBT:VBA$_4$ copolymer (1.0% AIBN) occurred at $t_{gel} = 46$ s of irradiation.

In addition, Figure 7(C) and (D) show the molecular weight evolution in function of the extent of reaction α for both copolymers. The behavior of the registered trends agrees with the results of the model which calculates the extent of reaction a as a function of the irradiation time. The predicted gel points for the VBT:VBA$_4$ copolymers 0.4% and 1.0% AIBN where $a_{gel} = 0.63$ and $a_{gel} = 0.77$, respectively.

The developed mathematical model allows to calculate the individual contribution from the inter- and intra-chain interactions to the global crosslinking degree a as time evolves. Figure 8 presents the hypothetical contribution of the inter- and intra-chain crosslinking interactions to the overall progress of the

reaction. It was observed that since the chains are shorter in the VBT:VBA$_4$ copolymer (1.0% AIBN) (Figure 8(B), red dash line), the extent of the intra-chain reaction increases, representing up to 82% of the global α. In contrast, for VBT:VBA$_4$ copolymer (0.4% AIBN) (Figure 8(A), red dash line) approximately 73% of thymine moieties are involved in intra-chain reactions.

5. Conclusions

In this study, two VBT:VBA$_4$ copolymers with 0.4% w/w AIBN and 1.% w/w AIBN were successfully synthesized and characterized. The characterization of the monomers and copolymer via ^{1}H NMR spectroscopy confirmed the identity of the products as well as their purity. GPC characterization method was used to determine the average molecular weights of the copolymers, and it was found that VBT:VBA$_4$ copolymers (0.4% w/w AIBN) have a higher molecular weight (Mw = 135,000) compared to VBT:VBA$_4$ copolymers (1.0% w/w AIBN) (Mw = 68,000).

The gel point of the copolymers was determined using results from UV–Vis and GPC spectroscopy, coupled with a mathematical model for the crosslinking process. The theoretical values for the gel point (t_{gel}) obtained with the **ESM** model showed a very good agreement with the UV–Vis and GPC spectroscopy experimental results for all VBT:VBA$_4$ copolymers studied. It was found that the gel point for the VBT:VBA$_4$ copolymer with 0.4% AIBN was shorter (t_{gel} = 24 s) compared to 1.0% AIBN (t_{gel} = 46 s). The results are consistent with the fact that longer chains (less AIBN present) will crosslink in a shorter time.

The mathematical model also allows to predict the contribution of inter- and intra-chain reactions to the global crosslinking. It was calculated that for the VBT:VBA$_4$ copolymer with 0.4% AIBN, nearly 73% of thymine moieties are involved in intra-chain reactions, whereas for 1.0% AIBN, the percentage is higher, basically 82%. These interesting results inspire the implementation of new studies using copolymers under different synthetic conditions in order to achieve a more solid conclusion. It is hoped that the new evidence will allow us to increase the functionalities of thymine-based copolymers, and extend their applications.

Acknowledgements

Disclosure statement

No potential conflict of interest was reported by the authors.

Funding

Notes on contributors

N. Chen graduated from Simmons College with a Bachelor of Science degree in Chemistry in 2015. After graduation, she worked at Jordi Labs in Mansfield, MA, for three years and gained experience in small molecules and polymer analysis. She is currently attending Northeastern University for her Master's degree in analytical chemistry.

Professor N. Lee was born in Seoul, South Korea, and her family immigrated to the U.S. when she was in middle school. She pursued chemistry at the University of Pennsylvania. With BS in chemistry, she worked in the pharmaceutical industry (Merck & Wyeth-Ayerst) for four years where she fell in love with synthetic organic chemistry. She attended Brown to get a Ph.D. in organic synthesis where she studied synthesis of vitamin D metabolites and analogs. After a year of postdoctoral work at MIT in organometallic chemistry, she came to Simmons. She has been teaching organic chemistry to science majors and prehealth majors since 1994. She worked on an interesting class of compounds originally isolated from sharks called squalamines which has clinical potential in controlling tumors as an anti-angiogenic agent. More recently, she has devoted her research on synthesis and characterization of green polymers.

Dr S. A. Bortolato was born in Rosario, Argentina. He obtained his BS and his Ph.D. in Chemistry from the School of Biochemical and Pharmaceutical Sciences, National University of Rosario. He is member of the National Research Council of Argentina (CONICET) at the Rosario Institute of Chemistry (IQUIR), Department of Analytical Chemistry, University of Rosario. He has published about 30 scientific papers in international journals and several books and book chapters.

Dr D. M. Martino was born in Reconquista, Argentina. She earned her BS/MS and Ph.D. in Physics at the National University of Rosario, Argentina, and performed her postdoc at the University of Massachusetts Boston. She was appointed as Adjunct Prof. at the University of Massachusetts Boston, and then as a research scientist at the Francis Bitter Magnet Laboratory at MIT. For 15 plus years Dr Martino has been a Professor at the Universidad Nacional del Litoral and a member of the National Research Council of Argentina (CONICET). Her rich background in research and academia includes more than 50 scientific papers in international journals and book chapters. In January 2015, Dr Martino joined the Warner Babcock Institute for Green Chemistry.

References

[1] Blackburn, G.M.; Davies, R.J.H. The Structure of DNA-derived Thymine Dimer. *Biochem. Biophys. Res. Commun.* **1966**, *22* (6), 704–706. doi:10.1016/0006-291x(66)90205-1. (B) Lamola, A.A.; Mittal, J.P. Solution Photochemistry of

Thymine and Uracil. *Science* **1966**, *154*(3756), 1560–1561. doi:10.1126/science.154.3756.1560.

[2] Yamada, H.; Hieda, K. Wavelength Dependence (150–290 nm) of the Formation of the Cyclobutane Dimer and the (6–4) Photoproduct of Thymine. *Photochem. Photobiol.* **1992**, *55*, 541–548.

[3] Takemoto, K. Functional Monomers and Polymers Containing Nucleic Acid Bases. *J. Polym. Sci. Polym. Symp.* **1976**, *55*, 105–125.

[4] Lutz, J.-F.; Thünemann, A.F.; Nehring, R. Preparation by Controlled Radical Polymerization and Self-Assembly via Base-Recognition of Synthetic Polymers Bearing Complementary Nucleobases. *J. Polymer Sci. A: Polymer Chem.* **2005**, *43*, 4805–4818.

[5] Imai, Y.; Ogoshi, T.; Naka, K.; Chujo, Y. Formation of IPN Organic-Inorganic Polymer Hybrids Utilizing the Photodimerization of Thymine. *Polym. Bull.* **2000**, *45*, 9–16.

[6] Dahman, Y.; Puskas, J.E.; Margaritis, A.; Merali, Z.; Cunningham, M. Novel Thymine-Functionalized Polystyrenes for Applications in Biotechnology. *Polymer Synthesis and Characterization, Macromolecules* **2003**, *36*, 2198–2205.

[7] Xu, H.; Hong, R.; Lu, T.; Uzun, O.; Rotello, V.M. Recognition-Directed Orthogonal Self-Assembly of Polymers and Nanoparticles on Patterned Surfaces. *J. Am. Chem. Soc.* **2006**, *128*, 3162–3163.

[8] Trakhtenberg, S.; Hangun-Balkir, Y.; Warner, J.; Bruno, F.; Kumar, J.; Nagarajan, R.; Samuelson, L. Photo-Cross-Linked Immobilization of Polyelectrolytes for Enzymatic Construction of Conductive Nanocomposites. *J. Am. Chem. Soc.* **2005**, *127*, 9100–9104.

[9] Grasshoff, J.; Taylor, L.; Warner, J. U. S., 1995.

[10] Grasshoff, J.; Taylor, L.; Warner, J. U. S., 1997.

[11] Grasshoff, J.; Taylor, L.; Warner, J. U. S., 1998.

[12] Warner, J.C.; Cannon, A.S.; Raudys, J.; Undurti, A. U. S., 2004.

[13] Inaki, Y. Thymine Polymers as High Resolution Photoresists and Reversible Photo-Recording Materials. *Polym. News* **1992**, *17*, 367–367.

[14] Trakhtenberg, S.; Warner, J.C.; Nagarajan, R.; Bruno, F.F.; Samuelson, L.A.; Kumar, J. Spectroscopic and Microscopic Analysis of Photo-Cross-Linked Vinylbenzylthymine Copolymers for Photoresist Applications. *Chem. Mater.* **2006**, *18*, 2873–2878.

[15] El-Hayek, R.F.; Dye, K.; Warner, J.C. Bacteriostatic Polymer Film Immobilization. *J. Biomed. Mater. Res. A* **2006**, *79A*, 874–881.

[16] Barbarini, A.L.; Estenoz, D.A.; Martino, D.M. Crosslinkable Micelles from Diblock Amphiphilic Copolymers Based on Vinylbenzyl Thymine and Vinylbenzyl Triethylammonium Chloride. *J. Appl. Polym. Sci.* **2015**, *132*, No. 19, 6146–6156.

[17] Saito, K.; Warner, J.C. Core-Shell Thymine Containing Polymeric Micelle System: Study of Controlled Release of Riboflavin. *Green Chem. Lett. Rev.* **2009**, *2*, 71–76.

[18] Kaur, G.; Chang, S.L.Y.; Bell, T.D.M.; Hearn, M.T.W.; Saito, K. Bioinspired Core-Crosslinked Micelles from Thymine-Functionalized Amphiphilic Block Copolymers: Hydrogen Bonding and Photo-Crosslinking Study. *J. Polymer Sci. A: Polymer Chem.* **2011**, *49*, 4121–4128.

[19] Whitfield, J.R.; Morelli, A.; Warner, J.C. Enzymatic Reversal of Polymeric Thymine Photocrosslinking with *E. Coli* DNA Photolyase. *J. Macromol. Sci. A* **2005**, *42*, 1541–1546.

[20] Paz Zanini, V.I.; Tulli, F.; Martino, D.M.; López de Mishima, B.; Borsarelli, C.D. Improvement of the Amperometric Response to ʟ-Lactate by Using a Cationic Bioinspired Thymine Polycation in a Bioelectrode with Immobilized Lactate Oxidase. *Sens. Actuat B: Chem.* **2013**, *181*, 251–258.

[21] Paz Zanini, V.I.; Gavilán, M.; López de Mishima, B.; Martino, D.M.; Borsarelli, C.D. A Highly Sensitive and Stable Glucose Biosensor Using Thymine-Based Polycations into Laponite Hidrogel Films. *Talanta* **2016**, *150*, 646–654.

[22] Mark, H.F. *Encyclopedia of Polymer Science and Technology*, Concise 3° ed., John Wiley & Sons, 2007.

[23] Winter, H.H.**2016**. Gel Point. In *Encyclopedia of Polymer Science and Technology*. Wiley. doi:10.1002/0471440264.pst476.pub2.

[24] Elkordy, A.A. *Applications of Calorimetry in a Wide Context – Differential Scanning Calorimetry, Isothermal Titration Calorimetry and Microcalorimetry*. InTech. 2013; p. 13. doi:10.5772/2898.

[25] Turi, E.A. *Thermal Characterization of Polymeric Materials*; Academic Press: New York, 1981.

[26] Flory, P.J. *Principles of Polymer Chemistry*; Cornell University Press: Ithaca, NY, 1953. Chap. 9; Stockmayer, W.H.; J. Chem. Phys. 1943, *11*, 45; J. Chem. Phys. 1944, *12*, 125.

[27] Miller, D.; Macosko, C. Molecular Weight Relations for Crosslinking of Chains with Length and Site Distribution. *J. Polym. Sci., Part B: Polym. Phys.* **1987**, *25*, 2441–2469.

[28] Miller, D.; Macosko, C. Network Parameters for Crosslinking of Chains with Length and Site Distribution. *J. Polym. Sci., Part B: Polym. Phys.* **1988**, *26*, 1–54.

[29] Barbarini, A.L.; Estenoz, D.A.; Martino, D.M. Synthesis, Characterization and Curing of Bioinspired Polymers Based on Vinyl Benzyl Thymine and Triethyl Ammonium Chloride. *Macromol. React. Eng.* **2010**, *4*, 453–459.

[30] Martino, D.M.; Reyna, D.; Estenoz, D.A.; Trakhtenberg, S.; Warner, J.C. Photosensitization of Bioinspired Thymine-Containing Polymers. *J. Phys. Chem. A* **2008**, *112*, No. 21, 4786–4792.

[31] Ledesma, J.; Bortolato, S.A.; Martino, D.M.; Boschetti, C.E. Fluorescence Spectroscopy and Multivariate Analysis as a Greener Monitoring Tool: Characterization of the Curing Kinetics of Bioinspired Polymers. *Green Chem. Lett. Rev.* **2015**, *8*, No. 2, 26–38.

[32] Casis, N.; Luciani, C.V.; Vich Berlanga, J.; Estenoz, D.A.; Martino, D.M.; Meira, G.R. Synthesis of "Bioinspired" Copolymers: Experimental and Theoretical Investigation on Poly(Vinyl Benzyl Thymine-co-Triethyl Ammonium Chloride). *Green Chem. Lett. Rev.* **2007**, *1*, 65–72.

[33] Sarmoria, C.; Miller, D.R. Spanning-tree Models for Af Homopolymerizations with Intramolecular Reactions. *Comput. Theor. Polym. Sci.* **2001**, *11*, 113–127.

[34] Al-Harthi, M.; Khan, M.J.; Abbasi, S.H.; Soares, J. Gradient Copolymers by ATRP in Semibatch Reactors: Dynamic Monte Carlo Simulation. *Macromol. React. Eng.* **2009**, *3*, 148–159.

[35] Al-Harthi, M. Masihullah, J.; Abbasi, S.H.; Soares, J. Dynamic Monte Carlo Simulation of ATRP in a Batch Reactor. *Macromol. Theory Simul.* **2009**, *18*, 307–316.

[36] MATLAB version 7.10.0. Natick, Massachusetts: The MathWorks Inc., 2010.